

Accurate determination of the far-infrared dispersion in SrTiO₃ by hyper-Raman spectroscopy

H. Vogt

Max-Planck-Institut für Festkörperforschung, Heisenbergstrasse 1, 7000 Stuttgart 80, Federal Republic of Germany

G. Rossbroich

II. Physikalisches Institut der Universität Köln, Zùlpicher Strasse 77, 5000 Köln 41, Federal Republic of Germany

(Received 26 May 1981)

We use the fluctuation-dissipation theorem to relate the hyper-Raman scattering efficiency of transverse and longitudinal-optical phonons to the infrared dielectric function $\epsilon(\Omega) = \epsilon'(\Omega) + i\epsilon''(\Omega)$. The relation is applied to SrTiO₃ at room temperature in order to clarify the discrepancies between various far-infrared reflectivity studies. We take advantage of the hyper-Raman selection rules allowing the observation of Raman-forbidden modes. $\epsilon''(\Omega)$ is derived from accurately measured hyper-Raman lines and combined with compatible infrared reflectivity data to give $\epsilon'(\Omega)$. Below 100 cm⁻¹ the dielectric dispersion can be adequately described by a classical dispersion formula with a quasi-harmonic-oscillator frequency of 87.9 cm⁻¹ and a single damping constant of 23.7 cm⁻¹. This approximation fails above 100 cm⁻¹.

I. INTRODUCTION

Far-infrared reflectivity studies of perovskites have played a pioneering role in our understanding of structural phase transitions.¹ They initiated the experimental search for soft modes.² The accuracy in determining the dielectric function, however, has been rather poor because of unusually broad reflection bands with power reflectivities near 1 and small phase shifts between incident and reflected light. Owing to the small penetration depth of the far-infrared radiation the influence of surface conditions also has to be taken into account. These unfavorable conditions can hardly be overcome by advanced infrared techniques, so that Raman scattering seems to be a more accurate and easier method.¹

Nevertheless, in a considerable number of perovskites optical modes of central importance are Raman forbidden by symmetry. Modulation techniques have been invented to circumvent this difficulty, such as electric-field-induced³ and temperature-derivative⁴ Raman spectroscopy. A more direct access to infrared-active, but Raman-inactive, modes is opened by hyper-Raman scattering.⁵ In this process two photons of the incident laser light are simultaneously annihilated to give rise to one scattered photon. If only one laser source of frequency ω_L is used, the scattered light has frequencies $2\omega_L \pm \Omega$, where Ω stands for the frequencies of the phonons annihilated or created, respectively. Thus hyper-Raman (HR) lines are found in the spectral neighborhood of the second harmonic $2\omega_L$. Since an odd number of photons is involved, the HR effect has the same parity selection rule as the one-photon infrared absorption. In principle all infrared-active modes are also HR active. Moreover, some types of "silent"

modes being both Raman and infrared forbidden become observable by HR spectroscopy.⁶

In this paper the fluctuation-dissipation or Nyquist theorem is used to relate the efficiency for one-phonon HR scattering to the infrared dielectric function $\epsilon(\Omega) = \epsilon'(\Omega) + i\epsilon''(\Omega)$. The relation is applied to the lowest-frequency transverse and to the highest-frequency longitudinal-optical mode of SrTiO₃ at room temperature. Our special aim is to obtain accurate values of $\epsilon(\Omega)$ in the most interesting frequency range of the ferroelectric soft mode below 150 cm⁻¹ in order to clarify the discrepancies between the results of various far-infrared reflectivity studies.^{2,7-10} The relative values of $\epsilon''(\Omega)$ derived from the HR spectrum are calibrated by means of Kramers-Kronig and Lydane-Sachs-Teller relations. The minimum far-infrared reflectivity compatible with our absolute values of $\epsilon''(\Omega)$ is calculated and compared with experimental data. Complementing our $\epsilon''(\Omega)$ with consistent results of Ref. 7 and carrying out a Kramers-Kronig transformation, we also obtain $\epsilon'(\Omega)$ below 150 cm⁻¹ with reasonable accuracy. Finally, we calculate the soft-mode self-energy from our $\epsilon(\Omega)$ and discuss it in terms of the quasi-harmonic-oscillator model.

II. THEORETICAL BACKGROUND

The *spectral* efficiency $S(\omega)$ for spontaneous light scattering is defined as spectral differential cross section per unit volume and can be written (cgs units) as¹¹

$$S(\omega) = \left(\frac{\omega}{c}\right)^4 V \frac{\langle |\hat{e} \cdot \vec{P}^{NL}|^2 \rangle_\omega}{|E_L|^2}. \quad (1)$$

Here, ω is the frequency of the scattered light, c the velocity of light in vacuum, V the scattering

volume, E_L the amplitude of the incident laser radiation, \hat{e} a dimensionless unit vector in the direction of the scattered electric field, and \vec{P}^{NL} the nonlinear polarization representing the source of the scattered light. The essential term in (1) is the power spectrum of P^{NL} denoted by the bracket with subscript ω . Following the notation of Hayes and Loudon¹² we have

$$\langle |P^{NL}|^2 \rangle_\omega \delta(\omega - \omega') = \langle P^{NL*}(\omega) P^{NL}(\omega') \rangle, \quad (2)$$

where $P^{NL}(\omega)$ is the complex Fourier component of P^{NL} at frequency ω and the average is taken over the probability distribution at thermal equilibrium.

In the case of one-phonon HR scattering $P^{NL}(\omega)$ is given by

$$P_i^{NL}(\omega) = \sum_{j,l} \left(\sum_{\sigma} \frac{\partial \chi_{ijl}^{(2)}}{\partial W_{\sigma}^*} W_{\sigma}^* + \sum_m \frac{\partial \chi_{ijl}^{(2)}}{\partial E_m^*} E_m^* \right) (E_L)_j (E_L)_l, \quad (3)$$

where i, j, l , and m refer to the three Cartesian coordinate axes and σ is the phonon number.

The third-rank tensor $\chi^{(2)}$ is the second-order susceptibility responsible for second-harmonic generation in the absence of inversion symmetry. W_{σ} is the normal coordinate of the HR-active phonon σ , while \vec{E} is the electric field associated with the longitudinal-optical phonons. The complex conjugates of W_{σ} and \vec{E} are used to indicate Stokes scattering.

The phonons of SrTiO₃ under consideration are triply degenerate F_{1u} modes. Their HR tensors $\partial \chi^{(2)}/\partial W_{\sigma}^*$, referring to displacements along the three cubic axes x, y , and z , have the form¹³

$$\begin{aligned} R_x &= \begin{pmatrix} a & b & b & 0 & 0 & 0 \\ 0 & 0 & 0 & 0 & 0 & b \\ 0 & 0 & 0 & 0 & b & 0 \end{pmatrix}, \\ R_y &= \begin{pmatrix} 0 & 0 & 0 & 0 & 0 & b \\ b & a & b & 0 & 0 & 0 \\ 0 & 0 & 0 & b & 0 & 0 \end{pmatrix}, \\ R_z &= \begin{pmatrix} 0 & 0 & 0 & 0 & b & 0 \\ 0 & 0 & 0 & b & 0 & 0 \\ b & b & a & 0 & 0 & 0 \end{pmatrix}. \end{aligned} \quad (4)$$

The last two indices of $\chi^{(2)}$ have been contracted to a single one ranging from 1-6. As the normal coordinate W_{σ} of a F_{1u} mode transforms like a vector, the expressions (4) also apply to the electro-optical tensor $\partial \chi^{(2)}/\partial E_m^*$.

Insertion of (3) and (4) into (1) shows that $S(\omega)$ is determined by the power spectra $\langle W_{\sigma} W_{\tau}^* \rangle_{\Omega}$,

$\langle E_m E_n^* \rangle_{\Omega}$, and $\langle W_{\sigma} E_m^* \rangle_{\Omega}$ taken at the HR shift $\Omega = 2\omega_L - \omega$. Using the fluctuation-dissipation theorem we get^{11,12}

$$\langle W_{\sigma} W_{\tau}^* \rangle_{\Omega} = \frac{\hbar V}{4\pi^2 N^2} [n(\Omega) + 1] \times \text{Im} \left(\frac{\Delta \epsilon_{\sigma}(\Omega)}{Z_{\sigma}^2} \delta_{\sigma\tau} - \frac{\Delta \epsilon_{\sigma}(\Omega) \Delta \epsilon_{\tau}(\Omega)}{Z_{\sigma} Z_{\tau} \epsilon(\Omega)} \frac{(\vec{\xi}_{\sigma} \cdot \vec{q})(\vec{\xi}_{\tau} \cdot \vec{q})}{q^2} \right),$$

$$\langle E_m E_n^* \rangle_{\Omega} = -\frac{4\hbar}{V} [n(\Omega) + 1] \frac{q_m q_n}{q^2} \text{Im} \left(\frac{1}{\epsilon(\Omega)} \right), \quad (5)$$

$$\langle W_{\sigma} E_m^* \rangle_{\Omega} = -\frac{\hbar}{\pi N} [n(\Omega) + 1] \frac{(\vec{\xi}_{\sigma} \cdot \vec{q}) q_m}{q^2 Z_{\sigma}} \text{Im} \left(\frac{\Delta \epsilon_{\sigma}(\Omega)}{\epsilon(\Omega)} \right).$$

N is the number of primitive cells in the scattering volume V , $n(\Omega)$ the Bose-Einstein population factor, \vec{q} the phonon wave vector, and Z_{σ} the effective charge. $\vec{\xi}_{\sigma}$ represents a dimensionless unit vector parallel to the dielectric polarization due to W_{σ} . $\epsilon(\Omega)$ is the infrared dielectric function, additively composed of the mode contributions $\Delta \epsilon_{\sigma}(\Omega)$:

$$\epsilon(\Omega) = \epsilon(\infty) + \sum_{\sigma} \Delta \epsilon_{\sigma}(\Omega), \quad (6)$$

where $\epsilon(\infty)$ stands for the electronic part of ϵ . Strictly speaking, Z_{σ} and $\Delta \epsilon_{\sigma}$ only refer to TO modes and have to be specified as transverse effective charge and transverse dielectric function, respectively.¹⁴ In the case of LO modes, however, they still must be used in (5) and are not to be replaced by their longitudinal analogs.

To simplify the following formulas let us consider the special scattering configurations of our experiments. The incident and scattered beams are parallel to the cubic axes x and z , respectively, so that the phonon wave vector \vec{q} points into the [101] direction. If both the incident and scattered light are polarized parallel to the y axis [scattering configuration: $x(yy)z$], only TO modes contribute to the HR spectrum. We have

$$S(\omega) = \frac{\hbar}{4\pi^2} \left(\frac{\omega}{c} \right)^4 \left(\frac{V}{N} \right)^2 |E_L|^2 [n(\Omega) + 1] \sum_{\sigma} \frac{|a_{\sigma}|^2}{Z_{\sigma}^2} \text{Im}(\Delta \epsilon_{\sigma}). \quad (7)$$

This relation will be applied to the soft-phonon region $\Omega < 150 \text{ cm}^{-1}$. The HR line, observed there, is remarkably strong compared to the other HR lines of SrTiO₃ and those of the alkali halides.¹⁵ According to (7) this is primarily due to the large HR polarizability a_{σ} . The influence of the effective charge is canceled because Z_{σ}^2 appears in the denominator as well as in $\Delta \epsilon_{\sigma}$.

For $\Omega < 150 \text{ cm}^{-1}$ we may safely assume that the sums in (6) and (7) are dominated by the soft-phonon contributions and the frequency dependence of the HR efficiency is given by

$$S(2\omega_L - \Omega) = A_{yy} [n(\Omega) + 1] \text{Im}[\epsilon(\Omega)], \quad (8)$$

where A_{yy} is regarded as independent of Ω . Above 150 cm^{-1} the influence of the other modes can no longer be neglected, and Eq. (8) only holds if the ratio $|a_\sigma|/Z_\sigma$ is the same for all infrared and HR

phonons.

In order to observe LO modes the scattering configuration has to be $x(yx)z$, $x(zx)z$, or $x((z,y)y)z$. For $x(zx)z$ we find

$$S(\omega) = \hbar \left(\frac{\omega}{c}\right)^4 |E_L|^2 [n(\Omega) + 1] \text{Im} \left\{ \left(-\frac{1}{\epsilon}\right) \left[2 |b_x^{e0}|^2 + \frac{1}{\pi} \left(\frac{V}{N}\right) \sum_{\sigma} \text{Re}(b_\sigma^* b_x^{e0}) \frac{\Delta\epsilon_\sigma}{Z_\sigma} + \frac{1}{4\pi^2} \left(\frac{V}{N}\right)^2 \left(\sum_{\sigma} |b_\sigma|^2 \frac{\Delta\epsilon_\sigma(\Delta\epsilon_\sigma - \epsilon)}{Z_\sigma^2} + \sum_{\sigma > \tau} \text{Re}(b_\sigma^* b_\tau) \frac{\Delta\epsilon_\sigma \Delta\epsilon_\tau}{Z_\sigma Z_\tau} \right) \right] \right\}, \quad (9)$$

where b_x^{e0} is an element of the electro-optical tensor defined by Eq. (3). We shall apply formula (9) only to the highest-frequency LO mode around 800 cm^{-1} . In this case all the dielectric functions $\Delta\epsilon_\sigma(\Omega)$ appearing in the expression behind $(-1/\epsilon)$ may be assumed as small, real, and slowly varying with frequency. Thus the frequency dependence of the HR efficiency is described by

$$S(2\omega_L - \Omega) = A_{xx} [n(\Omega) + 1] \text{Im} \left(-\frac{1}{\epsilon(\Omega)} \right) \quad (10)$$

with A_{xx} being nearly independent of Ω .

III. EXPERIMENTAL DETAILS AND RESULTS

The HR spectrum of SrTiO_3 for 90° scattering was first published in Ref. 15. The first observation of polaritons was reported by Denisov *et al.*¹⁶ Similar results as in Refs. 15 and 16 were obtained by Inoue *et al.*¹⁷

We have carefully remeasured the highest- and lowest-frequency HR line denoted by LO4 and TO1, respectively. We used the same single-channel technique as already described in detail in Ref. 15. Commercially available crystals (National Lead Company, Titanium Division, USA) were sawed and ground to cubic samples with (100) surfaces, the orientation being controlled by Laue patterns. As mentioned above, the incident and scattered beam were parallel to [100] axes, while the phonon wave vector was in the [101] direction. The line shapes of LO4 and TO1 were measured for various scattering configurations using polarizers for both the laser and scattered radiation. As we always observed the same line shapes, all polarizers were removed in order to get the maximum of HR intensity. Then the full spectral slit width could be decreased down to about 4 cm^{-1} , so that no deconvolution was necessary for analyzing the relatively broad profiles.

Our experimental results are presented in Fig. 1, where the HR intensity, in counts per second, has been plotted as a function of the HR shift $\Omega = 2\omega_L - \omega$. The full curves have been obtained by using Eqs. (8) and (10) and fitting the param-

eters of a classical dispersion formula⁷ for $\epsilon(\Omega)$ to the experimental points. In the case of TO1 only a single oscillator has to be taken into account and two parameters, i.e., mode frequency and damping constant, have to be adjusted. The profile of LO4, however, is sensitively influenced by all the three F_{1u} modes. Six parameters, in addition to those of TO1, are needed for an adequate description, i.e., mode frequencies, damping constants, and relative effective charges of TO2 and TO4. In Table I our parameters are compared with those of Ref. 7 derived from the far-infrared reflectivity spectrum. The numbering, symmetry, and spectral position of the eight different Γ phonons of SrTiO_3 are also explained there.

The crosses in Fig. 2 show $\epsilon''(\Omega) = \text{Im}\epsilon(\Omega)$ as

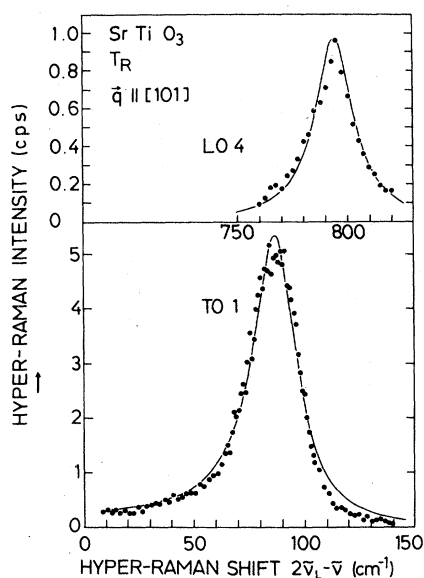


FIG. 1. Highest- and lowest-frequency hyper-Raman line of SrTiO_3 at room temperature (T_R). The hyper-Raman intensity is given in counts per second. The solid curves have been calculated from classical dispersion formulas with the parameters of Table I.

TABLE I. Dispersion parameters for SrTiO₃ at room temperature deduced from the hyper-Raman and the far-infrared reflectivity spectrum. Ω_0 is the mode frequency, γ the damping constant, Z the effective charge, HR represents hyper-Raman scattering in this work, and IR infrared reflection spectroscopy, Ref. 7.

Mode ^a	Symmetry	Ω_0 (cm ⁻¹) Reference 15	Classical dispersion analysis				$ Z/Z_1 $	
			HR	IR	HR	IR	HR	IR
TO1	F_{1u}	88	87.9	87.5; 87.7	23.7	26.3; 43.9	1	1
LO1		175						
TO2	F_{1u}	175	173.8	178	6.1	6.1; 6.9	0.22	0.22
LO2		266						
TO3	F_{2u} (silent)	266						
LO3		474						
TO4	F_{1u}	545	544.0	546; 544	18.0	26.8; 26.7	0.40	0.50; 0.44
LO4		795						

^a The numbering of the modes is in order of increasing frequencies.^{14,18} Note that LO3 corresponds to TO2, whereas LO2 and TO3 are degenerate and silent.

directly calculated from the TO1 HR line by means of Eq. (8). In order to calibrate the relative values, use is made of the Kramers-Kronig relation for the oscillator strength

$$\Delta\epsilon_1(0) = \frac{2}{\pi} \int_0^{\omega_1} \frac{\epsilon''(\Omega)}{\Omega} d\Omega, \quad (11)$$

where $\Delta\epsilon_1(0)$ is the contribution of TO1 to the static dielectric constant $\epsilon(0)$ and $\omega_1 \approx 150$ cm⁻¹ indicates the upper boundary of the TO1 frequency region. Since the modes of SrTiO₃ are clearly separated and the oscillator strength of TO1 is dominating,

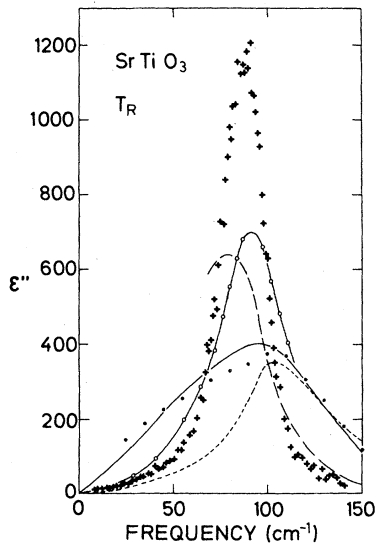


FIG. 2. The imaginary part of the dielectric function of SrTiO₃ at room temperature in the soft-mode-frequency region (crosses: this work, full line: Ref. 2, long dashes: Ref. 7, short dashes: Ref. 8, full circles: Ref. 9, full line with empty circles: Ref. 10).

the overlapping of $\Delta\epsilon_1''(\Omega)$ with the two other $\Delta\epsilon_s''(\Omega)$ may be neglected below 150 cm⁻¹.

$\Delta\epsilon_1(0)$ can be evaluated in two ways:

(a) According to Eq. (6) we have

$$\Delta\epsilon_1(0) = \frac{\epsilon(0) - \epsilon(\infty)}{1 + [\Delta\epsilon_2(0) + \Delta\epsilon_4(0)]/\Delta\epsilon_1(0)}. \quad (12)$$

The denominator can be estimated from the relative effective charges obtained by the classical dispersion analysis. $\epsilon(\infty) = 5.07$ follows from the refractive index at the minimum of dispersion around 5000 cm⁻¹.¹⁹ The Lyddane-Sachs-Teller (LST) relation¹⁴ allows us to calculate $\epsilon(0)$ from the exact mode frequencies measured by HR scattering.¹⁵ As shown in Table II the LST value is in satisfactory agreement with the results of other experimental techniques. From (12) we finally get $\Delta\epsilon_1(0) = 303$.

(b) $\Delta\epsilon_1(0)$ can also be estimated from the TO-LO splittings according to¹⁰

$$\Delta\epsilon_1(0) = \epsilon_\infty \left(\frac{\Omega_{LO1}^2 - \Omega_{TO1}^2}{\Omega_{TO1}^2} \right) \left(\frac{\Omega_{LO3}^2 - \Omega_{TO1}^2}{\Omega_{TO2}^2 - \Omega_{TO1}^2} \right) \left(\frac{\Omega_{LO4}^2 - \Omega_{TO1}^2}{\Omega_{TO4}^2 - \Omega_{TO1}^2} \right). \quad (13)$$

The result is $\Delta\epsilon_1(0) = 307$.

TABLE II. Static dielectric constant $\epsilon(0)$ of SrTiO₃ at room temperature as obtained by various experimental techniques.

Method	$\epsilon(0)$	References
Capacitance measurements at 1 kHz	307	20, 21
	315	22
"Magic T" at 0.3 cm ⁻¹	320	23
Reflectivity at 2.5 cm ⁻¹	322	2
Reflectivity at 5 cm ⁻¹	200	8
LST relation	313	15

Although the problem of mode coupling casts some basic doubts on the classical dispersion formula, the LST relation, and Eq. (13) (see, for instance, Ref. 24), the average value from (a) and (b), $\Delta\epsilon_1(0) = 305 \pm 10$, seems to be a reasonable approximation and is used in calibrating $\epsilon''(\Omega)$ by means of Eq. (11). Thus absolute values of $\epsilon''(\Omega)$ are deduced from the HR spectrum which are independent of infrared data.

In Fig. 2 we have also plotted the results of five available infrared works.^{2,7-10} In the three older ones,^{2,7,8} a grating spectrometer was employed, whereas in the two most recent ones Fourier spectroscopy in its symmetric¹⁰ and asymmetric⁹ version was used. Considerable discrepancies exist in the spectral region under study. According to our $\epsilon''(\Omega)$ the soft-phonon resonance seems to be much sharper than expected before.

In Fig. 3 the upper broken curve shows the minimum reflectivity compatible with our $\epsilon''(\Omega)$. There are only two measurements of the infrared reflectivity R (full triangles: Ref. 10, and crosses: Ref. 7) which are not clearly contradicted by the HR result. The lower broken curve presents the maximum phase shift between incident and reflected light as allowed by our $\epsilon''(\Omega)$. The experimental values of the phase shift ϕ determined by asymmetric Fourier spectroscopy⁹ are indicated by dots. They partly exceed the allowed maximum and hence are not confirmed by the HR spectrum. The full curves in Fig. 3 show R and ϕ as calculated from a classical dispersion formula with the parameters of Table I and $\Delta\epsilon_1(0) = 305$.

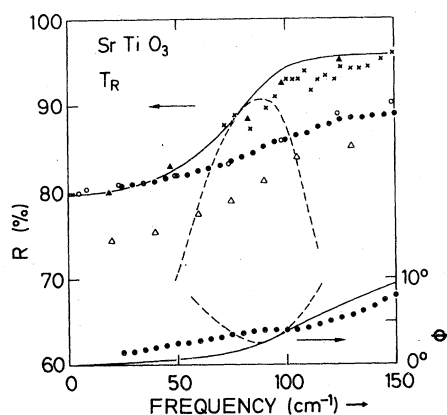


FIG. 3. Far-infrared power reflectivity R and phase shift ϕ of SrTiO_3 at room temperature (broken lines: minimum reflectivity and maximum phase shift compatible with the hyper-Raman data, solid lines: R and ϕ according to a classical dispersion formula, empty circles: Ref. 2, crosses: Ref. 7, empty triangles: Ref. 8, full circles: Ref. 9, full triangles: Ref. 10).

In order to get $\epsilon'(\Omega) = \text{Re}\epsilon(\Omega)$ for the soft-phonon region we may combine our $\epsilon''(\Omega)$ with the consistent reflectivity values of Refs. 7 and 10. The result is shown by the crosses and triangles in Fig. 4. It seems to be more accurate to deduce $\epsilon'(\Omega)$ from $\epsilon''(\Omega)$ by a Kramers-Kronig transformation after complementing our $\epsilon''(\Omega)$ with the values of Ref. 7 obtained for $\Omega > 150 \text{ cm}^{-1}$. We choose Ref. 7 because, according to Table I and Figs. 2 and 3, its results show the smallest deviations from ours. In Fig. 4 the solid curve represents $\epsilon'(\Omega)$ derived in this way. It partly coincides with the broken line showing the behavior of $\epsilon'(\omega)$ predicted by a classical dispersion formula.

IV. DISCUSSION

In Fig. 5 we have plotted the real and imaginary part of the soft-mode self-energy calculated from $\epsilon'(\Omega)$ (full curve in Fig. 4) and $\epsilon''(\Omega)$ (crosses in Fig. 2). We have followed the notation of Cowley^{9,22,25} writing the soft-mode contribution to $\epsilon(\Omega)$ as

$$\Delta\epsilon_f(\Omega) = \frac{\omega^h(0, f)^2 S_f(\Omega)^2}{\omega^h(0, f)^2 + 2\omega^h(0, f)D(0, f, \Omega) - \Omega^2}. \quad (14)$$

The index f is used instead of 1 for denoting the ferroelectric mode. $\omega^h(0, f)$ is the harmonic frequency at $q \approx 0$. $S_f(\Omega)^2$ and $D(0, f, \Omega)$ present the oscillator strength and complex self-energy, respectively.

In order to explain the instability of the soft mode the harmonic frequency $\omega^h(0, f)$ has been proposed to be imaginary.²⁵ The square of its

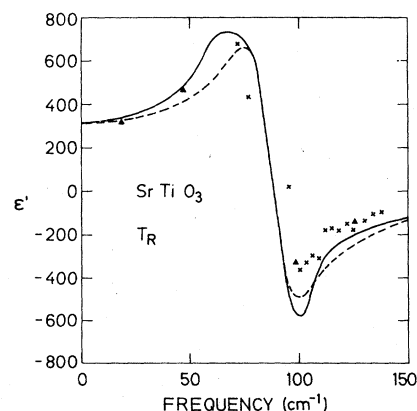


FIG. 4. The real part of the dielectric function of SrTiO_3 at room temperature in the soft-mode-frequency region [broken line: classical dispersion formula, solid line: Kramers-Kronig transformation from $\epsilon''(\Omega)$, points were calculated from R (crosses: Ref. 7, full triangles: Ref. 10) and $\epsilon''(\Omega)$ (crosses in Fig. 2)].

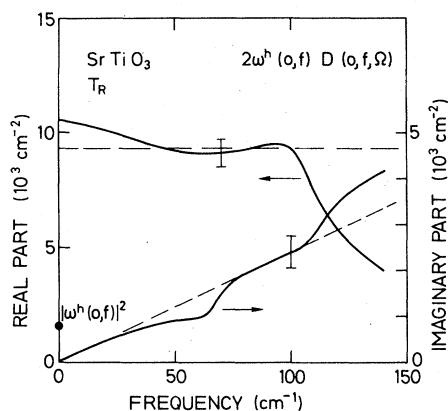


FIG. 5. Real and imaginary part of the soft-mode self-energy $2\omega^h(0,f)D(0,f,\Omega)$ of SrTiO_3 at room temperature. The value of the imaginary harmonic frequency was taken from Ref. 22 (broken lines: classical dispersion formula).

absolute value deduced by Lowndes and Rastogi²² is indicated at the left ordinate axis. $\omega^h(0,f)^2 < 0$ is highly overcompensated by the real part of $2\omega^h(0,f)D(0,f,\Omega)$. Thus the anharmonicity of the lattice potential energy provides the main contribution to the real quasiharmonic frequency.

Figure 5 confirms the picture already suggested by the lower half of Fig. 1: From the phenomenological point of view the ferroelectric soft mode of SrTiO_3 behaves like a classical oscillator with a single damping constant, although anharmonic interactions play a dominant role. The quasiharmonic-oscillator description, however, fails above 100 cm^{-1} .

ACKNOWLEDGMENTS

The authors wish to thank M. Cardona and W. Kress for stimulating discussions and reading the manuscript. The financial support by the Deutsche Forschungsgemeinschaft is gratefully acknowledged.

- ¹J. F. Scott, *Rev. Mod. Phys.* **46**, 83 (1974).
- ²A. S. Barker, Jr. and M. Tinkham, *Phys. Rev.* **125**, 1527 (1962).
- ³P. A. Fleury and J. M. Worlock, *Phys. Rev.* **174**, 613 (1968).
- ⁴Y. Yacoby, W. W. Krühler, and S. Just, *Phys. Rev. B* **13**, 4132 (1976).
- ⁵R. W. Terhune, P. D. Maker, and C. M. Savage, *Phys. Rev. Lett.* **14**, 681 (1965).
- ⁶S. J. Cyvin, J. E. Rauch, and J. C. Decius, *J. Chem. Phys.* **43**, 4083 (1965); D. A. Long and L. Stanton, *Proc. R. Soc. Lond.* **A318**, 441 (1970); D. L. Andrews and T. Thirunamachandran, *J. Chem. Phys.* **68**, 2941 (1978).
- ⁷W. G. Spitzer, R. C. Miller, D. A. Kleinman, and L. E. Howarth, *Phys. Rev.* **126**, 1710 (1962).
- ⁸C. H. Perry, B. N. Khanna, and G. Rupprecht, *Phys. Rev.* **135**, A408 (1964).
- ⁹K. F. Pai, T. J. Parker, N. E. Tornberg, R. P. Lowndes, and W. G. Chambers, *Infrared Phys.* **18**, 327 (1978); K. F. Pai, T. J. Parker, and R. P. Lowndes, *Ferroelectrics* **21**, 337 (1978).
- ¹⁰J. L. Servoin, Y. Luspin, and F. Gervais, *Phys. Rev. B* **22**, 5501 (1980).
- ¹¹A. S. Barker, Jr. and R. Loudon, *Rev. Mod. Phys.* **44**, 18 (1972).
- ¹²W. Hayes and R. Loudon, *Scattering of Light by Crystals* (Wiley, New York, 1978).
- ¹³S. W. Jha and J. W. F. Woo, *Nuovo Cimento* **2B**, 167 (1971).
- ¹⁴A. S. Barker, Jr., *Phys. Rev.* **145**, 391 (1966).
- ¹⁵H. Vogt and G. Neumann, *Phys. Status Solidi B* **92**, 57 (1979).
- ¹⁶V. N. Denisov, B. N. Mavrin, V. B. Podobedov, and Kh. E. Sterin, *Pis'ma Zh. Eksp. Theor. Fiz.* **31**, 111 (1980) [*JETP Lett.* **31**, 101 (1980)].
- ¹⁷K. Inoue and T. Sameshima, *J. Phys. Soc. Jpn.* **47**, 2037 (1979); K. Inoue, N. Asai, and T. Sameshima, *ibid.* **48**, 1787 (1980); **50**, 1291 (1981).
- ¹⁸R. A. Cowley, *Phys. Rev.* **134**, A981 (1964).
- ¹⁹W. L. Bond, *J. Appl. Phys.* **36**, 1674 (1965).
- ²⁰A. Linz, Jr., *Phys. Rev.* **91**, 753 (1953).
- ²¹G. A. Samara, *Phys. Rev.* **151**, 378 (1966).
- ²²R. P. Lowndes and A. Rastogi, *J. Phys. C* **6**, 932 (1973).
- ²³G. Rupprecht and R. O. Bell, *Phys. Rev.* **135**, A748 (1964).
- ²⁴A. S. Barker, Jr. and J. J. Hopfield, *Phys. Rev.* **135**, A1732 (1964).
- ²⁵R. A. Cowley, *Philos. Mag.* **11**, 673 (1965).